Biomed & Pharmacother 2000 ; 54 : 21-31

Dossier: 1999–2000 Special AIDS issue

Analysis of telomere length and thymic output in fast and slow/non-progressors with HIV infection

M.W. Richardson[1], A. Sverstiuk[1], H. Hendel[2], T.W. Cheung[3], J.F. Zagury[2], J. Rappaport[1]*

[1] *Center for NeuroVirology and Cancer Biology, Temple University, Philadelphia, PA, 19122 USA;* [2] *Laboratoire de Biologie Cellulaire, Université Pierre et Marie Curie, Paris, France;* [3] *UMDNJ New Jersey Medical School, Newark, NJ 07103, USA*

Summary – There are two models for CD4+ T-cell depletion leading to AIDS: a kinetic model and an immune suppression model. In the kinetic model, direct cell killing due to viral replication results in a continuous demand for CD4+ T-cells, which eventually exhausts their capacity for renewal by proliferative mechanisms. In the immune suppression model, CD4+ T-cell decline is due to an indirect global inhibitory effect of the virus on uninfected immune cell function. In order to address differences in the two models, we investigated proliferative history and thymic output in PBMC from the GRIV cohort of fast (FP) and slow/non-progressors (S/NP), and uninfected controls. Proliferative history and thymic output were assessed by measurement of mean telomeric restriction fragment (TRF) length and T-cell receptor Rearrangement Excision Circles (TREC) levels, respectively. Mean TRF lengths were significantly shorter in S/NP (n = 93, 7.59 ± 0.11 kb) and FP (n = 42, 7.25 ± 0.15 kb) compared to controls (n = 35, 9.17 ± 0.19 kb). Mean TRF length in PBMC (n = 9, 7.32 ± 0.31 kb) and CD4+ enriched fractions (n = 9, 7.41 ± 0.30 kb) from a subset of non-GRIV HIV-1 infected samples were also significantly smaller than PBMC (n = 8, 9.77 ± 0.33 kb) and CD4+ fractions (n = 8, 9.41 ± 0.32 kb) from uninfected controls. Rates of telomeric shortening, however, were similar among S/NP (n = 93, –45 ± 20 bp/yr), FP (n = 42, –41 ± 14 bp/yr) and controls (–29 ± 17 bp/yr). Paralleling differences observed in mean TRF length, TREC levels were significantly reduced in S/NP (n = 10, 3,433 ± 843 mol/μ and FP (n = 8, 1,193 ± 413) compared to controls (n = 15, 22,706 ± 5,089), indicative of a defect in thymopoiesis in HIV-1 infection. When evaluated in the context of reduced thymopoiesis, the difference in mean TRF length between S/NP and controls (1.58 ± 0.30 kb) is similar to that observed between memory and naïve T-cells (1.4 ± 0.1 kb), and may reflect perturbations in the peripheral T-cell population due to a decline in thymic output of naïve T-cells rather than increased turnover. Based on the different clinical criteria used to select S/NP and FP, the slight difference in TREC between these two groups suggests the threshold for pathogenesis as a result of naïve T-cell depletion may be quite low, and incremental increases in thymic output may yield substantial clinical results. Future studies regarding therapeutic vaccination, specifically with HIV-1 Tat targeted anti-immunosuppressive vaccines, should address the defect in thymic output in HIV-1 infection by using TREC analysis as a rapid method for biological evaluation. © 2000 Éditions scientifiques et médicales Elsevier SAS

HIV / telomeres / thymus

The natural course of HIV-1 infection involves CD4+ T-cell depletion, leading to opportunistic infection and death. Despite substantial investigation of the molecular pathogenesis of HIV-1 infection, controversy still exists regarding the mechanism by which HIV-1 infection leads to AIDS. Kinetic modeling studies suggest that there is a large and continuous demand for production of new CD4+ T-cells due to killing of target CD4+ T-cells by the virus. Progression to AIDS in the kinetic model occurs as the rate of elimination of CD4+ T-cells by the virus exceeds the rate of new CD4+ T-cell generation and eventually exhausts their capacity for renewal [1, 2]. Unfortunately, the relevance of this model is not clear as studies testing exhaustion of T-cell replicative capacity in progression to AIDS yielded conflicting results [3-8]. Furthermore, there is evidence that in adults the normal rate of production of naïve CD4+ T-cells is essentially an upper limit [9]. Viral interference with CD4+ T-cell renewal, perhaps by blocking proliferation or corrupting specialized lymphoid compartments [10], may be more relevant as a mechanism of CD4+ T-cell depletion.

Several lines of evidence now suggest that the decline in CD4+ T-cells in AIDS is ultimately a result of virally induced immune suppression, rather than a direct effect of cell killing and exhaustion of replicative capacity. In the immune suppression model, viral induced inhibition

*Correspondence and reprints: Jay Rappaport, Ph.D., Center for Neurovirology and Cancer Biology, Temple University, Philadelphia, PA 19122.

of uninfected immune cell function is a global effect. In agreement with this model, HIV-1-infected individuals exhibit a defect in T-cell proliferation even in the asymptomatic phase [11], perhaps due to an increase in activation-induced apoptosis [12-14], potentially reflecting the activity of soluble viral proteins [15, 16]. There is also a dramatic switch to a predominantly memory T-cell phenotype during HIV-1 infection [17-19], perhaps due to a significant decline in output of naïve T-cells from thymic or extrathymic peripheral lymphoid tissues [20]. HIV-1-induced suppression of thymopoiesis [21], primarily by an indirect cytopathic mechanism [22, 23], is likely responsible for the decline in thymic output.

Measurements of the length of telomeres, the ends of chromosomes, were employed previously to evaluate the proliferative history of T-cell populations in the context of HIV-1 infection. Telomeric measurements provided some evidence that proliferation-driven exhaustion of replicative capacity may not be particularly relevant to progression in HIV-1 infection [4, 8]. In humans, telomeres are primarily composed of approximately 3–12 kb of the distal tandem repeat $(TTAGGG)_n$ [24]. Telomeres decrease in length with age and proliferation in PBMC [25-27], in both naïve and memory T-lymphocytes [28], and in most cell types generally with the exception of the germ line [25, 28-32]. For reference, telomeres of adult human PBMC are roughly 9 kb in length on average [25-27, 31]. Telomere length, as quantified by measures of mean telomeric restriction fragment (TRF) length using oligo probes complementary to the distal repeat motif, is predictive of replicative capacity, and reflects replicative history [33]. Hence, mean TRF length in PBMC and T-cell subsets is a reasonable gauge of replicative history and therefore proliferation.

There is some controversy concerning the length of telomeres in CD4+ and CD8+ T-cells in the context of HIV-1 infection (for review see [34, 35]). It is fairly well accepted that telomeres of total PBMC and memory CD28– CD8+ T-cell subsets are significantly shorter in HIV-1-infected individuals relative to age-matched uninfected controls [3, 4, 6]. However, there are varying reports concerning the length of telomeres in CD4+ T-cells in HIV-1-infected individuals relative to controls. For example, a decrease in mean TRF length in CD4+ T-cells in symptomatic HIV-1-infected patients compared to controls was observed in two separate studies [6, 7]. However, another group found no difference in mean TRF length between HIV-1-infected individuals and controls in both unsorted CD4+ T-cells, and naïve and memory CD4+ T-cell subsets [4, 8]. Adding to the confusion, a third group reported an increase in mean TRF length in CD4+ cells from HIV-1-infected individuals relative to controls, although they did observe a substantial decrease in mean TRF length of CD8+ T-cells [5]. It is therefore uncertain whether preferential shortening of telomeres occurs in CD4+ T-cells relative to other lymphoid cell populations. Furthermore, it is questionable whether the observed reductions in mean TRF length, if true, are substantial enough to be indicative of massive senescence.

Analysis of mean TRF length, although perhaps a suitable marker for proliferation, does not permit discrimination between peripheral T-cell proliferation and the potential for an upstream blockade in T-cell production due to effects of the virus on, for example, thymic output of naïve T-cells. In HIV-1 infection, there is a switch to a predominantly memory CD4+ CD45RO+ T-cell phenotype due to a decline in naïve CD4+CD45RA+ T-cells [17, 18], and a similar decline in naïve CD8+ T-cells [19]. Recently, quantitative polymerase chain reaction (QC-PCR) assays for directly measuring thymic output were described [20, 36, 37]. The T-cell receptor rearrangement excision circle (TREC) assay measures thymic output by quantifying the amount of a stable excision product in circulating PBMC; the excision circle is produced by T-cell receptor gene rearrangement during development in the thymus and diluted out during subsequent proliferation in the periphery [36, 38, 39]. Using the TREC assay, a recent study demonstrated a significant impairment in thymic output in both CD4+ and CD8+ T-cells among HIV-1-infected individuals, even in the asymptomatic phase, which appears to be restored with therapeutic intervention [20]. In order to further explore the issues surrounding thymic output and telomeric length with respect to the mechanism of HIV-1 pathogenesis, we compared these two variables in fast and slow/non-progressors enrolled in the GRIV cohort in France.

The Genetic Resistance to Human Immunodeficiency Virus (GRIV) cohort was established in France to identify polymorphisms associated with non-progression to AIDS. Samples collected from 200 slow/non-progressors (S/NP) and 90 fast-progressors (FP) represent the extremes of clinical outcome in a population of 20,000 Caucasian HIV-1-infected patients of European descent (for review see [40]). To date, several factors associated with slow/non-progression have been identified in GRIV S/NP. For example, the frequency of the Δ32 deletion in the CCR-5 chemokine receptor is significantly higher in GRIV S/NP compared to both GRIV FP [41], and the general Caucasian

population [42]. There is also a higher frequency of mutation in the CCR-2 and SDF-1 receptors among S/NP compared to FP [42]. The HLA class I alleles B14 and C8 are enriched in S/NP, whereas the A29 and B22 alleles are more prevalent in FP [43]. Additionally, antibody to the HIV-1 early regulatory protein Tat is elevated in S/NP relative to FP [44].

Here we present our analysis of the GRIV cohort using measurements of mean TRF length and TREC levels as indicative of proliferation and thymic output, respectively. We also were interested in examining these two parameters in S/NP and FP to provide insight into mechanisms contributing to slow/non-progression in HIV-1 infection. Because GRIV genomic DNA samples are currently only available from patient PBMC, additional HIV-1 seropositive samples were obtained from volunteers outside the GRIV cohort and separated into both PBMC- and CD4+-enriched populations; a subset of controls was separated identically. In an effort to further address proliferation in CD4+ T-cells in the context of HIV infection, the PBMC- and CD4+-enriched subsets were examined for differences in mean TRF length.

MATERIALS AND METHODS

Patient samples

Uninfected control samples were collected with informed consent at Mt. Sinai Medical Center, New York, NY, and MCP-Hahnemann University Hospital, Philadelphia, PA, and were primarily drawn from Caucasian individuals. In addition to controls, HIV-1 seropositive samples were collected at Mt. Sinai, again with informed consent, and were separated into PBMC- and CD4+-enriched populations using anti-CD4 M450 DynaBeads (Dynal). HIV-1 seropositive samples obtained at Mt. Sinai from infectious disease and hemodialysis patients were drawn from a more racially diverse group of individuals, and generally did not meet the criteria for AIDS. HIV-1 seropositive slow/non-progressors (S/NP) and fast-progressors (FP) PBMC samples were obtained from the GRIV cohort in France, a uniformly Caucasian cohort. GRIV S/NP were selected based on the criteria of being HIV-1 seropositive and asymptomatic for more than eight years, and a CD4+ cell count > 500 x 10^6/mL[3] despite having no antiretroviral therapy. GRIV FP were HIV-1 seropositive with a CD4+ cell count < 300 x 10^6/mL[3] less than three years after seroconversion regardless of pharmacotherapeutic regimen; few received highly active antiretroviral therapy (HAART) due to its availability at the time of collection [40, 41]. For all samples, PBMC were separated initially from whole blood by Ficoll gradient sedimentation. Genomic DNA was isolated from control PBMC collected at MCP-Hahneman University using a QiaBlood kit (Qiagen); these samples were exclusively used as controls in the TREC assay, and were used in addition to controls from Mt. Sinai for mean TRF measurements. Genomic DNA was isolated from GRIV PBMC using hot phenol extraction; GRIV samples used in TREC analysis were further purified using QiaSpin columns (Qiagen) with elution at 55° C. Genomic DNA was isolated from PBMC- and CD4+-enriched populations collected at Mt. Sinai by overnight digestion at 55° C with proteinase K (Boehringer Mannheim), subsequent RNase A digestion at 37° C for 30 min, removal of cellular proteins by precipitation with high salt (6 M NaCl), and subsequent phenol/chloroform extraction, isopropanol precipitation, multiple washes with 70% ethanol and resuspension in TE buffer (10 mM Tris pH 8.0, 1 mM EDTA pH 8.0).

Telomeric length analysis

DNA ladders (10 μg each, Gibco-BRL) of five kilobase pair (kb) and 1 kb were labeled as described by the manufacturer using T4 DNA polymerase (New England Biolabs) and 50 mCi ^{32}P-∞ATP (NEN-Dupont), purified using G25 spin columns (5'–3', Inc.), and quantitated using a scintillation counter (Beckman). The labeled 5 kb (10^5 cpm) and 1 kb (4 x 10^5 cpm) ladders were used as molecular weight standards, with the 1 kb ladder loaded on both sides of the gel. Genomic DNA (2.5 μg) was digested overnight at 37° C in 50 μl with 20 U each of RsaI and HinfI and 1X buffer 2 (New England Biolabs). Samples were loaded on (l)25 cm x (w)20 cm 0.5% agarose (SeaKem, FMC) gels containing 1X TBE. Electrophoresis was performed for approximately 1,000 Volt-hours (Vhrs). Gels were denatured, neutralized, dried and hybridized essentially as previously described [45]. Briefly, gels were gently rocked for 30 min in denaturation buffer (0.5 N NaOH, 0.15 M NaCl), and for 30 min in neutralization buffer (0.5 M Tris-HCL, pH 8.0, 0.15 M NaCl). Gels were then placed on 3MM paper (Whatman), covered with plastic wrap and dried at 55° C for 2.5 h using a heated vacuum gel dryer (BioRad). Dried gels were soaked in deionized ultra pure water (Hydro) for 5 min to detach them from the 3MM paper and plastic wrap, placed in separate heat seal bags (Kaypak), and pre-hybridized for 2 h at 40° C in a rotating Belly Dancer incubator (Stovall) in 15 mL of pre-hyb buffer (6X SSC, 5X Denhardts, 50 mM $NaHPO_4$ pH 7.0, 0.1 mg/mL sonicated herring sperm DNA). One hundred ng of oligo 5'-$(C_2TAA)_3$-3' was end-labeled using polynucleotide kinase (New England Biolabs) and 50 μCi ^{32}P-γATP (NEN-Dupont), purified using a G25 spin column (5'–3', Inc.), and quantitated using a scintillation counter (Beckman). Gels were hybridized at 40° C

for 18 h with 1 x 10^6 cpm/mL of oligo probe in 20 mL of pre-hybridization buffer in a rotating Belly-Dancer incubator (Stovall). Hybridized gels were washed 3 x 10 min in 3X SSC at 40° C, exposed for 18 h to Phosphorimager screens (BioRad or Molecular Dynamics) and analyzed using ImageQuaNT software (Molecular Dynamics).

PhosphorImager analysis was performed essentially as previously described [4]. Small differences in migration from one side of the gel to the other, and any slant of the gel image caused by placement on the phosphorimager screen were compensated for by drawing a line connecting the radiolabeled 7 kb standards on either side; this line was then duplicated and copies set at heights of approximately 35 kb and 1 kb. Wide lines were drawn over each lane from 35 kb to 1 kb, adjusted to mirror any angle of the gel and placed flush with the identical 35 kb and 1 kb lines originally drawn by connecting the 7 kb standards. Area reports were performed for each lane, and the peak of each profile quantitated in mm. Peaks were treated as equivalent to mean telomeric repeat fragment (TRF) lengths, as previously described [4, 46]. 5 kb and 1 kb standards were quantitated identically. Distance of standard migration in mm and known size in kbp were plotted on the x- and y-axis, respectively, using Excel software (Microsoft). Tailed curves were fit between the 4 kb and 12 kb standards on each gel by power regression in Excel (all R^2 values > 0.98), and the equation derived from the curve used to calculate mean TRF length in kb for each sample on the gel. Mean TRF length and corresponding age were entered in Excel 4.0 spreadsheets (Microsoft) prior to import into SPSS 9.0 (SPSS, Inc.) for subsequent statistical analysis.

TREC analysis

TREC assays were performed as previously described [20]. Primers for signal-joint TREC [47] were as follows: 5'-aaagagggcagccctctccaaggcaaa-3' and 5'-aggctgatcttgtctgacatttgctccg-3'. A signal joint internal standard (10^2, 10^3 or 10^4 molecules) modified to be 60 bp shorter than the actual signal-joint TREC was added to each reaction [20]. PCR reactions were performed with 0.1–0.2 μg of PBMC genomic DNA under the following conditions previously established as being within the linear range of the assay: 95° C for 5 min, then depending upon the amount of standard added, 30 or 35 cycles of 95° C, 60° C and 72° C, each for 30 sec [20]. PCR reactions contained 1 U platinum Taq polymerase (Gibco-BRL), 1.8 mM $MgCl_2$, 0.2 mM dNTPs (New England Biolabs), 12.5 μM of each primer and 1.7 nmol (5 μCi) ^{32}P-labelled dCTP in 50 μL platinum Taq buffer. Reactions were run on 6% non-denaturing polyacrylamide 1X TBE gels for approximately 750 Vhrs. Gels were transferred to 3MM chromatography paper (Whatman) and dried for 45 min at 65° C using a vacuum gel dryer (BioRad). Gels were exposed to Phosphorimager screens for 18 h and then quantitated using a PhosphorImager and ImageQuaNT software (Molecular Dynamics). The amount of TREC for each sample was calculated by dividing the target sample signal joint intensity by the internal signal-joint standard intensity (corrected for lower GC content by multiplying by a factor of 1.156) and then multiplying by the number of signal-joint standard molecules added to the reaction [20].

Statistical analysis

Statistical analysis was performed using SPSS 9.0 (SPSS, Inc.) for Windows (Microsoft), after importing data from Excel 4.0 (Microsoft) spreadsheets. In all cases, the data appeared normally distributed by the Kolmogorov-Smirnov test for normality, with respect to both age and mean TRF length or TREC measurements. There did, however, appear to be a trend toward a difference in age within the GRIV cohort, with the GRIV SNP somewhat older than GRIV FP, as might be expected based on the inclusion criteria. The difference in age was more pronounced between GRIV SNP and GRIV FP samples used in the TREC analysis. It is important to note, though, that both mean TRF length and TREC decline with age, and that both measurements were lower among the younger GRIV FP rather than the older GRIV SNP. Hence, correction for differences in age would presumably only magnify the observed differences between GRIV SNP and GRIV FP with respect to both mean TRF length and TREC. Based on the apparent normality of each data set with respect to age and mean TRF length or TREC measurement, and the desire to control for age in some fashion, the parametric statistical procedure ANCOVA was performed using age as the covariate, followed by post-hoc comparisons with Bonferroni corrections when there were more than two groups and comparisons between individual group members were made; *P*-values from Bonferroni corrections are expressed in adjusted scales with $\alpha = 0.05$. Additionally, because some skewness was observed in the smaller data sets, the non-parametric-based procedures Kruskal-Wallis, Mann-Whitney or Wilcoxon-Signed Rank were performed to confirm significance observed with parametric procedures, and mirrored the ANCOVA results.

RESULTS AND DISCUSSION

In order to evaluate replicative history and, by inference, proliferation in GRIV S/NP and FP relative to uninfected controls, measurements of mean TRF length in PBMC were performed essentially as previously

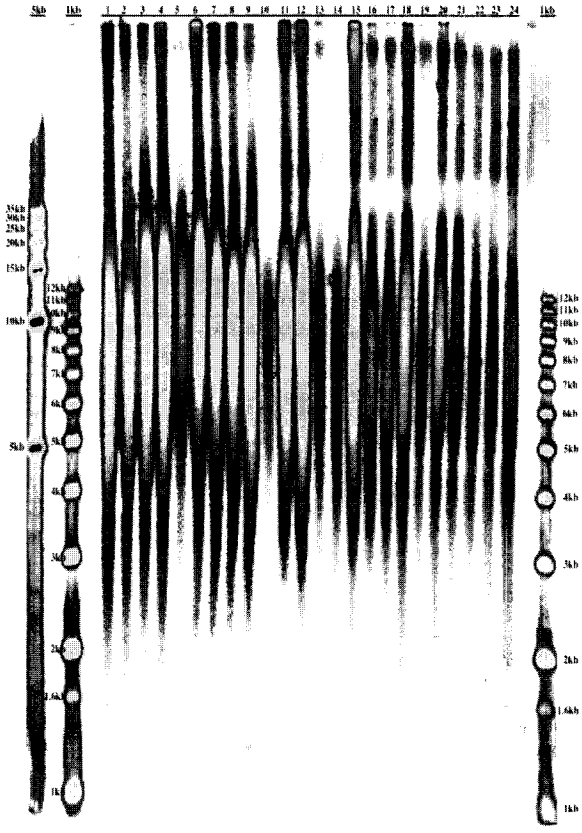

Figure 1. PhosphorImager scan of a gel representative of the in-gel Southern blot hybridization technique used to measure mean telomeric restriction fragment (TRF) length in HinfI and RsaI digested genomic DNA from both PBMC and CD4+ enriched populations. In-gel Southern blot hybridizaiton, PhosphorImager analysis and calculation of mean TRF lengths were performed as described in the Materials and Methods section.

Table I. Reproducibility and low variability of mean TRF length measurements by repeated assay of identical samples on separate gels.

Group	*Mean TRF (kb) ± SEM*	*SD*	*Number*
Control PBMC	9.73 ± 0.24	0.42	n = 3
GRIV S/NP PBMC	8.0 ± 0.20	0.28	n = 2
GRIV FP PBMC	7.45 ± 0.35	0.5	n = 2
HIV– Control PBMC	10.2 ± 0.10	0.14	n = 2
HIV– Control CD4+	9.95 ± 0.15	0.21	n = 2
HIV+ PBMC	6.75 ± 0.35	0.5	n = 2
HIV+ CD4+	6.8 ± 0.10	0.14	n = 2

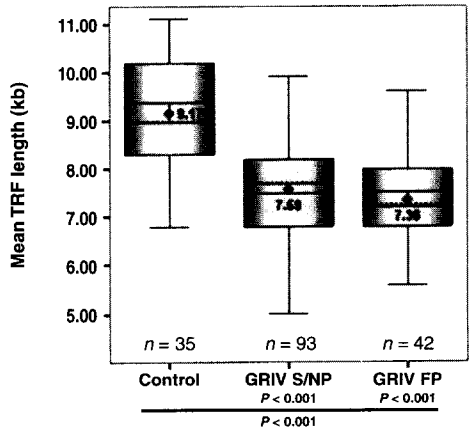

Figure 2A. There is a significant difference in mean TRF length between S/NP, FP and controls as a group ($P < 0.001$). Mean TRF length is significantly lower in both S/NP ($P < 0.001$) and FP ($P < 0.001$) when compared individually to controls. The mean of each group is marked in the box-plots with a diamond, and the numeric value is given. Solid lines within boxes represent the standard error of the mean. Dashed lines within boxes indicate the median. The upper and lower boundaries of the boxes represent the 75th and 25th percentiles, respectively. Whiskers represent the range of the values observed in each group.

described [4, 46], and as detailed in the Materials and Methods section. A representative gel is shown in *figure 1*; reproducibility and low variability of mean TRF length is demonstrated in *table I.* The Kolmogorov-Smirnov test for normality was performed for each group separately with respect to both age and mean TRF length. Ages and mean TRF lengths were normally distributed for all three groups. Although there was no significant difference in the mean ages for the three groups by ANOVA, differences in mean TRF length were evaluated using ANCOVA, with age as the covariate, in order to eliminate any effect due to age. By ANCOVA, there was a significant difference in mean TRF length of PBMC between S/NP (n = 93, 7.59 ± 0.11 kb), FP (n = 42, 7.25 ± 0.25 kb), and controls (n = 35, 9.17 ± 0.19 kb) as a group ($P < 0.001$) *(figure 2A, table II).* The mean TRF lengths of S/NP ($P < 0.001$), and FP ($P < 0.001$) were significantly reduced when compared to controls individually *(figure 2A, table II).*

Cross-sectional analysis of age and mean TRF length by scatter plot, linear regression and Pearson's correlation is shown in *figure 2B*, and reveals a significant inverse relationship between age and mean TRF length when all three groups are combined ($P < 0.001$). Within groups, there was a significant correlation between age and mean TRF in controls (P = 0.032) and in S/NP (P = 0.003), and a trend toward significance in FP (P = 0.085) *(figure 2B, table II).* Rates of mean TRF length shortening calculated for each group by cross-sectional analysis (controls = –45 ± 20 bp/yr; S/NP = –41 ± 14 bp/yr; FP = –29 ± 17 bp/yr) are shown in *table II*, and agree with previous cross-sectional

Table II. Mean TRF lengths, ANCOVA age-adjusted mean TRF lengths, rates of decline in mean TRF length with age, and Pearson's correlation between mean TRF length and age for controls, S/NP and FP.

Group	*N*	*Mean TRF (kb) ± SEM*	*ANCOVA Mean TRF*	*SD*	*ANCOVA*	*Rate (bp/yr)*	*Pearson (TRF/age)*
Control	35	9.17 ± 0.19	9.12 ± 0.17	1.15	–	(–45) ± 20	$P = 0.032$
GRIV S/NP	93	7.59 ± 0.11	7.64 ± 0.11	1.07	$P < 0.001$	(–41) ± 14	$P = 0.003$
GRIV FP	42	7.25 ± 0.15	7.29 ± 0.16	0.98	$P < 0.001$	(–29) ± 17	$P = 0.085$

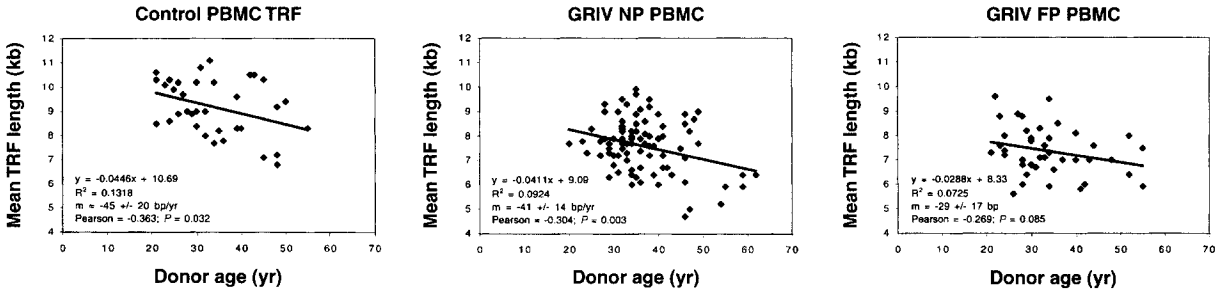

Figure 2B. Scatter plots and linear regressions of age vs mean TRF length for controls, S/NP and FP. There was a significant correlation between age and mean TRF length when all groups were combined ($P < 0.001$), and separately in controls ($P = 0.032$), and S/NP ($P = 0.003$); although there was no significant correlation between age and mean TRF length in GRIV FP, there was a similar trend ($P = 0.085$). Cross-sectional calculation of the annual rate of decrease in mean TRF length revealed no significant differences between groups. The similarities in slopes suggest that there may not be significant differences in proliferation between the three groups.

estimates of approximately –30 to –50 bp/yr [26, 32, 48]. The rates of telomeric shortening were surprisingly similar for all groups despite quite different mean TRF lengths. To explain the apparent discrepancy between the similarity in rates of telomeric shortening and the differences in telomeric lengths, we propose that the decrease in mean TRF length in HIV-1-infected individuals is due primarily to a shift in the composition of the T-cell population rather than increased proliferation. It is important to note however that cross-sectional analysis may be less powerful than longitudinal analysis because of variability in mean TRF length in different individuals, although this limitation may be compensated for in our study by relatively large sample size.

To address past controversy concerning mean TRF length in CD4+ T-cells in the context of HIV-1 infection, we measured mean TRF length in both PBMC- and CD4+-enriched fractions from a group of non-GRIV HIV-1-infected individuals and a subset of controls. Each group was determined to be normally distributed with respect to both age and mean TRF length using the Kolmogorov-Smirnov test for normality. By ANCOVA, there was no difference in mean TRF length between PBMC- (n = 8, 9.85 ± 0.33 kb) and CD4+-enriched (n = 8, 9.43 ± 0.32 kb) fractions within controls *(figure 3)*. Similarly, there was no difference between

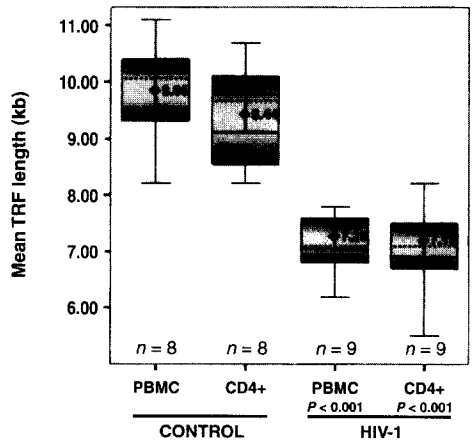

Figure 3. Mean TRF lengths of PBMC- and CD4+-enriched populations from controls and non-GRIV HIV-1 seropositive samples. There was no significant difference in mean TRF length between PBMC- and CD4+-enriched populations within either group. However, mean TRF length was significantly lower in both PBMC- and CD4+-enriched populations from HIV-1 seropositive samples compared to controls ($P = 0.001$). The mean of each group is given and is indicated graphically with a diamond; solid lines within each box represent the standard error of the mean. Dashed lines within each box denote the median. The upper and lower boundaries of each box represent the 75th and 25th percentiles of the observed values, respectively. Whiskers show the range of the values observed in each group.

Table III. Mean TRF length and ANCOVA age-adjusted mean TRF length of PBMC- and CD4+-enriched populations from controls and non-GRIV HIV-1 seropositive individuals.

Group	*N*	*Mean TRF (kb) ± SEM*	*ANCOVA Mean TRF (kb)*	*SD*	*ANCOVA*
Overall Control PBMC	35	9.17 ± 0.19	9.12 ± 0.17	1.15	–
Control PBMC	8	9.85 ± 0.33	9.77 ± 0.33	0.91	–
Control CD4+	8	9.43 ± 0.32	9.41 ± 0.32	0.92	–
HIV+ PBMC	9	7.29 ± 0.31	7.33 ± 0.31	0.84	$P < 0.001$
HIV+ CD4+	9	7.19 ± 0.30	7.41 ± 0.30	0.74	$P = 0.001$

Table IV. Mean TREC values, ANCOVA age-adjusted mean TREC values, mean TRF lengths, and ANCOVA age-adjusted mean TRF lengths of controls, S/NP and FP.

Group	*N*	*Mean TREC (mol/μg) ± SEM*	*ANCOVA Mean TREC*	*SD*	*ANCOVA*
Control	15	22,706 ± 5,089	22,190 ± 3,297	19,710	–
GRIV S/NP	10	3,433 ± 843	6,971 ± 4,330	2,665	$P = 0.030$
GRIV FP	8	1,193 ± 413	(–2,264) ± 4,763	1,166	$P = 0.001$
Group	*N*	*Mean TRF (kb) ± SEM*	*ANCOVA Mean TRF*	*SD*	*ANCOVA*
Control	15	9.05 ± 0.25	9.03± 0.25	0.96	–
GRIV S/NP	10	7.95 ± 0.30	8.08 ± 0.32	1.08	$P = 0.085$
GRIV FP	8	7.78 ± 0.34	7.65 ± 0.36	0.75	$P = 0.009$

PBMC- (n = 9, 7.29 ± 0.31 kb) and CD4+-enriched (n = 9, 7.19 ± 0.30 kb) fractions from HIV-1-infected individuals. However, as shown in *figure 3*, mean TRF length in PBMC from HIV-1 infected individuals was significantly shorter than in controls ($P < 0.001$), in agreement with previous reports [3, 4]. Mean TRF length in CD4+-enriched fractions from HIV-1-infected individuals was also significantly reduced compared to controls ($P < 0.001$), in agreement with some previous studies [6, 7], but not others [4, 5, 8].

At first glance, decreased mean TRF length in PBMC from S/NP and FP, and in both PBMC- and CD4+-enriched fractions from non-GRIV HIV-1 positive samples would seem to reflect an increase in proliferation, possibly supporting exhaustion of replicative capacity as a mechanism in AIDS. However, the decrease in mean TRF length is not substantial enough in either PBMC or CD4+ cells to indicate massive senescence, which is typically associated with mean TRF lengths below 5 kb [7]. Furthermore, the rates of telomeric shortening are essentially identical in S/NP (–41 ± 14 bp/yr), FP (–29 ± 17 bp/yr) and controls (–45 ± 20 bp/yr) as shown in *figure 2B*. Our results in CD4+ cells do not support an alternative hypothesis that increased production of naive CD4+ T-cells from either the thymus or extra-thymic sources occurs, and leads to a net increase in mean TRF length [4, 5]. In fact, the apparent increase in proliferation, as quantified by a decrease in mean TRF length, may better reflect a decrease in thymic output and hence reliance on existing memory cells. In support of this hypothesis, although telomeres decrease in length with proliferation in both naive and memory T-lymphocytes [28], mean TRF lengths of both memory CD8+ T-cells and memory CD4+ T-cells are approximately 1.4 ± 0.1 kb shorter than their naive counterparts [28, 49]. We observed a comparable decrease in mean TRF length in S/NP (1.58 ± 0.30 kb) relative to controls, in FP (1.92 ± 0.34 kb), and in non-GRIV HIV-1 seropositive PBMC (1.85 ± 0.5 kb) compared to control PBMC overall (n = 35). Our results are therefore consistent with a blockade in naive T-cell production and an increase in the relative proportion of memory cells in the peripheral circulation. Taken together, our results do not support the theory of proliferative exhaustion of CD4+ T-cells as a relevant mechanism for AIDS pathogenesis.

In order to evaluate thymic output both as a determinant of HIV-1 infection and disease progression, and as a variable affecting mean TRF length as a gauge of proliferation, TREC analysis using QC-PCR was performed as previously described [20], and as detailed in the Materials and Methods section. A phosphorimager scan of a gel representative of the TREC QC-PCR technique employed in TREC analysis is shown in *figure 4A*. TREC values and age were determined to be normally distributed using the Kolmogorov-Smirnov test for normality. By ANCOVA, there was a significant difference in the level of TREC between GRIV S/NP (n = 10, 3,433

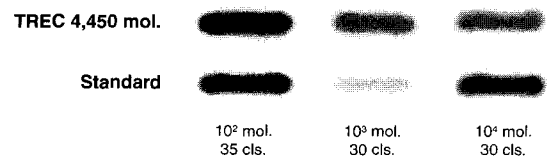

Figure 4A. PhosphorImager scan of a gel representative of TREC analysis, performed as described in the Materials and Methods section. Upper bands represent amplification of signal joint TREC from an experimental sample, quantified as 4,450 mol/μg based on calculations performed using the values of the lower bands, the signal-joint standards, as detailed in the Materials and Methods section.

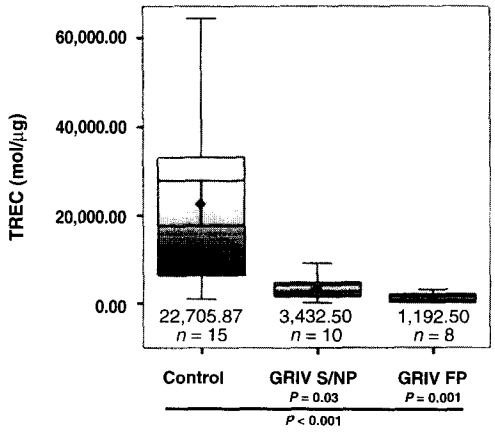

Figure 4B. There is a significant difference in mean TREC levels (mol/μg) among S/NP, FP and controls as a group ($P < 0.001$). Mean TREC values are significantly lower in S/NP ($P = 0.03$), and in FP ($P = 0.001$) compared to controls. TREC values in S/NP and FP were not significantly different, although TREC levels were lower in FP. As in previous box-plots, the mean of each group is indicated with a diamond and the numeric value is given. Solid lines within each box represent the standard error of the mean. Dashed lines within each box denote the median. The upper and lower boundaries of each box represent the 75th and 25th percentiles, respectively. Whiskers show the range of the values observed in each group.

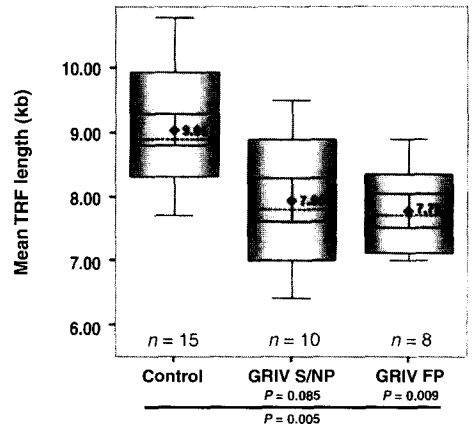

Figure 4C. Box-plot of mean TRF length in controls, S/NP and FP used in the TREC analysis. Mirroring the TREC results, there was a significant difference in mean TRF length among controls, S/NP and FP ($P = 0.005$) as a group. Mean TRF length was significantly lower for FP compared to controls ($P = 0.009$). Although the decrease in mean TRF length among S/NP compared to controls was not significant, there was a trend toward significance ($P = 0.085$).

± 843), GRIV FP ($n = 8$, 1,193 ± 413) and controls ($n = 15$, 22,706 ± 5,089) as a group, ($P < 0.001$) *(figure 4B)*. As shown in *figure 4B*, TREC was significantly lower in both S/NP ($P = 0.03$), and in FP ($P = 0.001$), compared to controls. There was no significant difference in TREC between S/NP and FP, although TREC was lower in FP; significance may be observed with larger sample size. It will be interesting to evaluate more thoroughly in future studies whether there is in fact a difference in thymic output between S/NP and FP, and perhaps by longitudinal analysis to determine if the decline in thymic output is more abrupt in FP, as would perhaps seem to be implied by their selection criteria. Although we did not examine TREC in CD4+-enriched subsets, a previous report demonstrated reduced levels of TREC in both CD8+ and CD4+ T-cells from HIV-1-infected individuals [20]. Hence, when this information is combined with evidence of a switch to a predominantly memory T-cell phenotype due to a decline in naive CD4+CD45RA+ T-cells [17, 18], and a similar decline in naive CD8+ T-cells [19], it seems increasingly unlikely that there is a separate reservoir for naive CD4+ T-cells compared to CD8+ T-cells, as has been suggested [4].

As shown in *figure 4C*, there was a similar decrease in mean TRF length among the S/NP and FP samples used in the TREC analysis as observed in S/NP and FP overall *(figure 4C)*. By ANCOVA, there was a significant difference in mean TRF length between S/NP, FP and controls as a group ($P = 0.005$). Although the mean TRF length of S/NP was not significantly smaller than that of controls ($P = 0.085$), there was certainly a trend toward significance which would likely be achieved given a larger sample size. We did observe a significant difference in mean TRF length between FP and controls ($P = 0.009$). Hence, similar results were obtained in terms of mean TRF length for the subset of GRIV samples used in the TREC analysis as were observed among GRIV overall; the S/NP TREC subset mean TRF length was approximately 1.1 ± 0.55 kb smaller, and the FP subset 1.3 ± 0.59 kb smaller compared to controls. There was a significant correlation between TREC lev-

els and mean TRF length in S/NP, FP and controls as a group ($P = 0.042$), and separately in FP ($P = 0.04$) and controls ($P = 0.048$), but interestingly not S/NP. Abrogation of naive T-cell influx into the periphery from the thymus may explain in large part the observed decrease in mean TRF length in both S/NP and FP compared to controls. Although more substantial decreases were observed in analysis of mean TRF length in non-GRIV HIV-infected samples, when non-GRIV HIV-1 seropositive PBMC mean TRF lengths were compared to controls overall ($n = 35$), the difference was less dramatic (1.85 ± 0.5 kb); the control sample size used in the PBMC/CD4+ subset analysis was relatively small and values obtained may reflect higher variability. Still, it is not possible to exclude an increase in proliferation completely, although certainly there is evidence that although T-cells from HIV-1-infected individuals express activation antigens in response to HIV-1 antigens, they fail to proliferate, even in the asymptomatic phase [11].

CONCLUSIONS

Our results are in good agreement with recent evidence of a substantial defect in thymic output in the context of HIV-1 infection [20], which is likely responsible for the switch to a predominantly CD4+ CD45RO+ memory phenotype [17, 18], and the decline in naive CD8+ T-cells observed in HIV-1 infection [19]. Our data support the conclusion that a defect in thymic output leads to perturbations in peripheral T-cell populations; a net reduction in telomeric length occurs as the T-cell population shifts to a principally memory phenotype [28, 49]. The similarity in telomeric shortening rates, together with the observed defect in thymic output, do not support the increase in T-cell turnover which has been proposed to lead to AIDS. In this light, the HIV-1 regulatory protein Tat is emerging as a viral toxin with potent immunosuppressive properties [50]. Tat induces apoptosis in human T-cells [15, 51-53], and blocks their proliferation upon antigen stimulation [54-56]. Hence it is possible that Tat may play a role in HIV-1-induced suppression of thymopoiesis [21], by indirect cytopathic mechanisms [22, 23]. Furthermore, resistance of HIV-1-infected chimpanzees to progression to AIDS may reflect the apparent resistance of chimpanzee T-cells to HIV-1 Tat-induced apoptosis [57]. Based on the known biological properties of HIV-1 Tat, as well as the correlation between anti-Tat antibodies and clincial stability in the GRIV cohort [44], a rationale exists for the development of Tat-targeted vaccines [58, 59]. Based on the different criteria used to select S/NP and FP, the slight difference in TREC between these two groups suggests that the threshold for pathogenesis as a result of naive T-cell depletion may be quite low, and incremental increases in thymic output may yield substantial clinical results. Future studies regarding therapeutic vaccination, specifically with HIV-1 Tat-targeted anti-immunosuppressive vaccines, should focus attention on potential increases in thymic output as a rapid method for biological evaluation.

AKCNOWLEDGEMENTS

We would like to extend our sincere thanks to: Dr. Danny Douek at the University of Texas Southwestern Medical Center, Dallas, TX, for procedures and discussions regarding the TREC assay; Dr. Jaime Uribarrie at the Mount Sinai Medical Center, Division of Renal Diseases and Hypertension, New York, NY, for kindly providing clinical samples; Dr. Edward Gracely at MCP-Hahnemann University, Philadelphia, PA, for helpful discussions and review of statistical methods; and finally Dr. Rosyln Gorin at Temple University, Philadelphia, PA, also for helpful statistical discussions. This work was supported by NIH grants to JR.

REFERENCES

1 Ho DD, Neumann AU, Perelson AS, Chen W, Leonard JM, Markowitz M. Rapid turnover of plasma virions and CD4 lymphocytes in HIV-1 infection. Nature 1995 ; 373 : 123-6.
2 Wei X, Ghosh SK, Taylor ME, Johnson VA, Emini EA, Deutsch P, et al. Viral dynamics in human immunodeficiency virus type 1 infection. Nature 1995 ; 373 : 117-22.
3 Effros RB, Allsopp R, Chiu CP, Hausner MA, Hirji K, Wang L, et al. Shortened telomeres in the expanded CD28-CD8+ cell subset in HIV disease implicate replicative senescence in HIV pathogenesis. AIDS 1996 ; 10 : F17-22.
4 Wolthers KC, Bea G, Wisman A, Otto SA, De Roda Husman AM, Schaft N, et al. T cell telomere length in HIV-1 infection: no evidence for increased CD4+ T cell turnover. Science 1996 ; 274 : 1543-7.
5 Palmer LD, Weng NP, Levine BL, June CH, Lane HC, Hodes RJ. Telomere length, telomerase activity, and replicative potential in HIV infection: analysis of CD4+ and CD8+ T cells from HIV-discordant monozygotic twins. J Exp Med 1997 ; 185 : 1381-6.
6 Pommier JP, Gauthier L, Livartowski J, Galanaud P, Boue F, Dulioust A, et al. Immunosenescence in HIV pathogenesis. Virology 1997 ; 231 : 148-54.
7 Nichols WS, Schneier S, Chan RC, Farthing CF, Daar ES. Increased CD4+ T-lymphocyte senescence fraction in advanced human immunodeficiency virus type 1 infection. Scand J Immunol 1999 ; 49 : 302-6.
8 Wolthers KC, Noest AJ, Otto SA, Miedema F, DeBoer RJ. Normal telomere lengths in naïve and memory CD4+ T Cells in HIV type I infection: a mathematical interpretation. AIDS Res Hum Retrovir 1999 ; 15 : 1053-62.
9 Mackall CL, Fleisher TA, Brown MR, Andrich MP, Chen CC, Feuerstein IM, et al. Age, thymopoiesis, and CD4+ T-lymphocyte regerneration after intensive chemotherapy. N Engl J Med 1995 ; 332 : 143-9.

10 Zhang ZQ, Notermans DW, Sedgewick G, Cavert W, Wietgrefe S, Zupancic M, et al. Kinetics of CD4+ T cell repopulation of lymphoid tissues after treatment of HIV-1 infection. Proc Natl Acad Sci USA 1998 ; 95 : 1154-9.
11 Caruso A, Licenziati S, Canaris AD, Corulli M, De Francesco MA, Cantalamessa A, et al. T Cells from individuals in advanced stages of HIV-1 infection do not proliferate but express activation antigens in response to HIV-1-specific antigens. J Acquir Immune Defic Syndr Hum Retrovirol 1997 ; 15 : 61-9.
12 Groux H, Torpier G, Monte D, Mouton Y, Capron A, Ameisen JC. Activation-induced death by apoptosis in CD4+ T cells from human immunodeficiency virus-infected asymptomatic individuals. J Exp Med 1992 ; 175 : 331-40.
13 Gougeon ML, Garcia S, Heeney J, Tschopp R, Lecoeur H, Guetard D, et al. Programmed cell death in AIDS-related HIV and SIV infections. AIDS Res Hum Retrovir 1993 ; 9 : 553-63.
14 Meyaard L, Otto SA, Jonker RR, Mijnster MJ, Keet RP, Miedema F. Programmed death of T cells in HIV-1 infection. Science 1992 ; 257 : 217-9.
15 Li CJ, Friedman DJ, Wang C, Metelev V, Pardee AB. Induction of apoptosis in uninfected lymphocytes by HIV-1 Tat protein. Science 1995 ; 268 : 429-31.
16 Zagury, JF, Chams V, Carcagno M, Rappaport J, Bizzini B, Burney A. Model of AIDS immunopathogenesis based on the HIV-1 gp120 and Tat-induced dysregulation of uninfected immune cells. Cell Pharm AIDS Sci 1996 ; 3 : 123-8.
17 Sleasman JW, Aleixo LF, Morton A, Skoda-Smith S, Goodenow MM. CD4+ memory T cells are the predominant population of HIV-1-infected lymphocytes in neonates and children. AIDS 1996 ; 10 : 1477-84.
18 Ullum H, Lepre AC, Victor J, Skinhoj P, Phillips AN, Pedersen BK. Increased losses of CD4+CD45RA+ cells in late stages of HIV infection is related to increased risk of death: evidence from a cohort of 347 HIV-infected individuals. AIDS 1997 ; 11 : 1479-85.
19 Roederer M, Dubs JG, Anderson MT, Raju PA, Herzenberg LA. CD8 naïve T cell counts decrease progressively in HIV-infected Adults. J Clin Invest 1995 ; 95 : 2061-6.
20 Douek DC, McFarland RD, Keiser PH, Gage EA, Massey JM, Haynes BF, et al. Changes in thymic function with age and during the treatment of HIV infection. Nature 1998 ; 396 : 690-5.
21 Bonyhadi ML, Rabin L, Salimi S, Brown DA, Kosek J, McCune JM, et al. HIV induces thymus depletion in vivo. Nature 1993 ; 363 : 728-32.
22 Su L, Kaneshima H, Bonyhadi M, Salimi S, Kraft D, Rabin L, et al. HIV-1-induced thymocyte depletion is asociated with indirect cytopathogenicity and infection of progenitor cells in vivo. Immunity 1995 ; 2 : 25-36.
23 Koka PS, Jamieson BD, Brooks DG, Zack JA. Human immunodeficiency virus type 1-induced hematopoietic inhibition is independent of productive infection of progenitor cells In vivo. J Virol 1999 ; 73 : 9087-9.
24 Moyzis RK, Buckingham JM, Cram LS, Dani M. A highly conserved repetitive DNA sequence, (TTAGGG)n, present at the telomeres of human chromosomes. Proc Natl Acad Sci USA 1988 ; 85 : 6622-6.
25 Hastie ND, Dempster M, Dunlop MG, Thompson AM, Green DK, Allshire RC. Telomere reduction in human colorectal carcinoma and with ageing. Nature 1990 ; 346 : 866-8.
26 Vaziri H, Schachter F, Uchida I, Wei L, Zhu X, Effros R, et al. Loss of telomeric DNA during aging of normal and trisomy 21 human lymphocytes. Am J Hum Genet 1993 ; 52 : 661-7.
27 Slagboom PE, Droog S, Boomsma DI. Genetic determination of telomere size in humans: a twin study of three age groups. Am J Hum Genet 1994 ; 55 : 876-82.
28 Weng NP, Levine BL, June CH, Hodes RJ. Human naive and memory T lymphocytes differ in telomeric length and replicative potential. Proc Natl Acad Sci USA 1995 ; 92 : 11091-4.
29 Lindsey J, McGill NI, Lindsey LA, Green DK, Cooke HJ. In vivo loss of telomeric repeats with age in humans. Mutat Res 1991 ; 256 : 45-8.
30 Counter CM, Avilion A, LeFeuvre CE, Stewart NG, Greider CW, Harley CB, et al. Telomere shortening associated with chromosome instability is arrested in immortal cells which express telomerase activity. EMBO J 1992 ; 11 : 1921-9.
31 Allshire RC, Dempster M, Hastie ND. Human telomeres contain at least three types of G-rich repeats distributed nonrandomly. Nucleic Acids Res 1989 ; 17 : 4611-27.
32 Vaziri H, Dragowsk W, Allsopp RC, Thomas TE, Harley CB, Lansdorp PM. Evidence for a mitotic clock in human hematopoietic stem cells: loss of telomeric DNA with age. Proc Natl Acad Sci USA 1994 ; 91 : 9857-60.
33 Allsopp RC, Vazirir H, Patterson C, Goldstein S, Younglai EV, Futcher AB, et al. Telomere length predicts replicative capacity of human fibroblasts. Proc Natl Acad Sci USA 1992 ; 89 : 10114-8.
34 Effros RB, Pawelec G. Replicative senescence of T cells: does the Hayflick Limit lead to immune exhaustion? Immunol Today 1997 ; 18 : 450-4.
35 Wolthers KC, Schuitemaker H, and Miedema F. Rapid CD4+ t-cell turnover in HIV-1 infection: a paradigm revisited. Immunol Today 1998 ; 19 : 44-8.
36 Kong FK, Chen CH, Cooper MD. Thymic function can be accurately monitored by the level of recent T cell emigrants in the circulation. Immunity 1998 ; 8 : 97-104.
37 Kong FK, Chen CH, Six A, Hockett RD, Cooper MD. T cell receptor gene deletion circles identify recent thymic emigrants in the peripheral T cell pool. Proc Natl Acad Sci USA 1999 ; 96 : 1536-40.
38 Livak F, Schatz D. T-cell receptor locus V(D)J recombination by-products are abundant in thymocytes and mature t cells. Mol Cell Biol 1996 ; 16 : 609-18.
39 Takeshita S, Toda M, Yamagishi H. Excision products of the T-cell receptor gene support a progressive rearrangment model of the alpha/delta locus. EMBO J 1989 ; 8 : 3261-70.
40 Hendel H, Cho YY, Gauthier N, Rappaport J, Schachter F, Zagury JF. Contribution of cohort studies in understanding HIV-1 pathogenesis: introduction of the GRIV cohort and preliminary results. Biomed Pharmacother 1996 ; 50 : 480-7.
41 Rappaport J, Cho YY, Hendel H, Schwartz E, Schachter F, Zagury JF. 32bp CCR5 gene deletion and resistance to fast progression in HIV-1 infected heterozygotes. Lancet 1997 ; 349 : 922-3.
42 Hendel H, Henon N, Le Buanec H, Lachgar A, Poncelet H, Caillat-Zucman S, et al. Distinctive effects of CCR5, CCR2, and SDF1 genetic polymorphisms in AIDS progression. J Acquir Immune Defic Syndr Hum Retrovirol 1998 ; 19 : 381-6.
43 Hendel H, Caillat-Zucman S, LeBuanec H, Carrington M, O'Brien S, Andrieu JM, et al. New class I and II HLA alleles strongly associated with opposite patterns of progression to AIDS. J Immunol 1999 ; 162 : 6942-6.
44 Zagury JF, Sill A, Blattner W, Lachgar A, Le Buanec H, Richardson M, et al. Antibodies to the HIV-1 Tat protein correlated with nonprogression to AIDS: a rationale for the use of Tat toxoid as an HIV-1 vaccine. J Human Virol 1998 ; 1 : 282-92.

45 Ehtesham NZ, Hasnain SE. Direct in-gel hybridization without blotting, using nick-translated cloned DNA probe. Bio Techniques 1991 ; 11 : 718-21.
46 Oexle K. Telomere length distribution and southern blot analysis. J Theor Biol 1998 ; 190 : 369-77.
47 Verschuren, MC, Wolvers-Tettero IL, Breit TM, Noordzij J, Van Wering ER, Van Dongen JJ. Preferential rearrangements of the T-cell receptor-delta-deleting elements in human T cells. J Immunol 1997 ; 158 : 1208-16.
48 Harley CB, Futcher AB, Greider WC. Telomeres shortendur-ing ageing of human fibroblasts. Nature 1990 ; 345 : 458-60.
49 Monteiro J, Batliwalla F, Ostrer H, Gregersen PK. Shortened telomeres in clonally expanded CD28-CD8+ T cells imply a replicative history that Is distinct from their CD28+CD8+ counterparts. J Immunol 1996 ; 156 : 3587-90.
50 Zagury D. A naturally unbalanced combat. Nat Med 1997 ; 3 : 156-7.
51 McCloskey TW, Ott M, Tribble E, Khan SA, Teichberg S, Paul MO, et al. Dual role of HIV Tat in regulation of apoptosis in T cells. J Immunol 1997 ; 158 : 1014-19.
52 Westendorp MO, Frank R, Ochsenbauer C, Stricker K, Dhein J, Walczak H, et al. Sensitization of T cells to CD95-mediated apoptosis by HIV-1 Tat and gp120. Nature 1995 ; 375 : 497-500.
53 Katsikis PD, Garcia-Ojeda ME, Torres-Roca JF, Greenwald DR, Herzenberg LA, Herzenberg LA. HIV type 1 Tat protein enhances activation-but not Fas (CD95)-induced peripheral blood T cell apoptosis in healthy individuals. Int Immunol 1997 ; 9 : 835-41.
54 Viscidi RP, Mayur K, Lederman HM, Frankel AD. Inhibition of antigen-induced lymphocyte proliferation by Tat protein from HIV-1. Science 1989 ; 246 : 1606-8.
55 Zagury JF, Lachgar A, Bizzini B, Astgen A, Lecoq H, Fouchard M, et al. A critical role of Tat and IFNa in the HIV-1 induced immunosuppression leading to AIDS. Cell Pharm AIDS Sci 1996 ; 3 : 104-8.
56 Chirmule N, Than S, Khan SA, Pahwa S. Human immunodeficiency virus Tat induces functional unresponsiveness in T cells. J Virol 1995 ; 69 : 492-8.
57 Ehret A, Westendorp MO, Herr I, Debatin KM, Heeney JL, Frank R, et al. Resistance of chimpanzee T cells to human immunodeficiency virus type 1 Tat-enhanced oxidative stress and apoptosis. J Virol 1996 ; 70 : 6502-7.
58 Gringeri A, Santagostine E, Muca-Perja M, Mannucci PM, Zagury JF, Bizzini B, et al. Safety and immunogenicity of HIV-1 Tat Toxoid in immunocompromised HIV-1 infected patients. J Hum Virol 1998 ; 1 ; 293-8.
59 Gringeri A, Santagostino E, Muca-Perja M, Le Buanec H, Bizzini B, Lachgar A, et al. Tat toxoid as a component of a preventive vaccine in seronegative subjects. J Acquir Immune Defic Syndr Hum Retrovirol 1999 ; 20 ; 371-5.